

# Force and Compliance Measurements on Living Cells Using Atomic Force Microscopy (AFM)

Ewa P. Wojcikiewicz,<sup>1</sup> Xiaohui Zhang<sup>1</sup> and Vincent T. Moy<sup>1\*</sup>

<sup>1</sup>Department of Physiology and Biophysics, University of Miami School of Medicine, Miami, FL 33136, USA.

\*To whom correspondence should be addressed: Vincent T. Moy, Department of Physiology and Biophysics, University of Miami School of Medicine, 1600 NW 10<sup>th</sup> Avenue, Miami, FL 33136 USA. Tel: 305–243–3201; Fax: 305–243–5931; Email: vmoy@miami.edu

Submitted: September 23, 2003; Revised: October 17, 2003; Accepted: December 10, 2003; Published: January 15, 2004.

Indexing terms: Cell adhesion; Leukocytes; Microscopy, Atomic Force.

Abbreviations: atomic force microscope, AFM; leukocyte function-associated antigen-1, LFA-1; intercellular adhesion molecule-1, ICAM-1; phorbol myristate acetate, PMA.

---

## ABSTRACT

We describe the use of atomic force microscopy (AFM) in studies of cell adhesion and cell compliance. Our studies use the interaction between leukocyte function associated antigen-1 (LFA-1)/intercellular adhesion molecule-1 (ICAM-1) as a model system. The forces required to unbind a single LFA-1/ICAM-1 bond were measured at different loading rates. This data was used to determine the dynamic strength of the LFA-1/ICAM-1 complex and characterize the activation potential that this complex overcomes during its breakage. Force measurements acquired at the multiple-bond level provided insight about the mechanism of cell adhesion. In addition, the AFM was used as a microindenter to determine the mechanical properties of cells. The applications of these methods are described using data from a previous study.

---

## INTRODUCTION

Interactions between ligands and receptors are crucial for the proper function of living organisms. For example, the human body's immune response is largely dependent on the adhesion of leukocytes to target cells. The leukocyte function associated antigen-1 (LFA-1) is the principle receptor used by lymphocytes to bind to the ICAM family of ligands. LFA-1 is composed of an  $\alpha_L$  and  $\beta_2$  chain, and it binds most strongly to intercellular adhesion molecule-1 (ICAM-1) found on the target cells (1). In Wojcikiewicz *et al.*, we reported on studies of this receptor-ligand interaction carried out with LFA-1-expressing 3A9 cells and the

ICAM-1 protein (2, 3). In the past, studies of ligand-receptor interactions usually involved biochemical methods of binding affinities or rate constants. This type of data contributes greatly to our understanding of protein-protein interactions, but it provides little information about the influence of internal and external forces that affect plasma membrane receptors. In the body, these forces can include the internal stress of migrating cells undergoing cycles of adhesion and de-adhesion and external perturbations due to blood flow currents that are experienced by lymphocytes attached to blood vessel walls. Recently, the development of techniques such as atomic force microscopy (AFM) has made it possible for us to acquire measurements that reveal the mechanical properties of biomolecules under applied

force. Here we focus on the use of the AFM in measuring ligand-receptor interactions. Also included are detailed methods and experimental protocols that can be applied toward studying most protein-protein interactions.

The AFM was originally designed as an imaging tool, but was later modified to be operated in the force scan mode (4). Its high sensitivity makes it possible to measure interactions between two opposing surfaces down to the single molecule level. In studies of ligand-receptor forces, the ligand can be immobilized on the surface of a flexible AFM cantilever while the receptor is attached to a suitable substrate. The deflection of the cantilever during the approach and withdrawal of the cantilever from the substrate allow for the force of the interaction to be measured. Lee *et al.* were able to directly measure the unbinding force of a single ligand-receptor interaction using this method (5). This novel application led to the use of the AFM as an ultra-sensitive force transducer for probing biomolecular interactions. This non-imaging AFM technique has also been used to study the unfolding of individual proteins in recent years (6, 7).

AFM force measurements of ligand-receptor interactions can be used to determine the dynamic strength of a complex and characterize the changes in free energy that the particular complex undergoes (i.e., energy landscape) during its breakage. The Bell model can be used to interpret these measurements (8). The Bell model is based on the assumption that the application of an external mechanical force to a receptor-ligand interaction bond will reduce the activation energy that needs to be overcome in order to break this bond. This unbinding force should increase with the logarithm of the rate at which an external mechanical force is applied toward the unbinding of adhesion complexes (i.e., loading rate). This was confirmed by a number of studies. For example, studies using the biomembrane force probe (BFP) (8) and the AFM have shown that increases in loading rate cause an increase in rupture force between individual complexes of streptavidin/biotin (10, 11).

The AFM can also be used in adhesion studies involving whole cells (11). In these studies we examine the interaction between a cell expressing a particular receptor of interest and its ligand protein or another cell expressing the ligand. The cell adhesion experiments allow for the acquisition of both single-molecule measurements, like in the above-mentioned studies, as well as multiple-bond interactions. The advantage of using the AFM in cell adhesion studies is the high specificity and wealth of information that is obtained. The AFM force scans provide information about the individual bond strengths as well as the force and work that is required to separate the entire complex. Combining single molecule and multiple-bond data allows us to describe the thermodynamic model of the separation of a particular complex in addition to the mechanism of its action on the cellular scale (2, 3).

In our recent study, the AFM was used for a dual purpose. It served as a pulling device to detach adherent cells from protein-coated surfaces and obtain measurements of the single and multiple-bond protein-protein interactions. The AFM also

served as a microindenter that probed the cells revealing information about their mechanical properties. This type of information, which cannot be obtained using standard cell biological methods, allowed us to estimate Young's modulus of living 3A9 cells. This report summarizes the AFM techniques used in the Wojcikiewicz *et al.* study (2).

## METHODS

### Cells and reagents

The 3A9 cell line was maintained in continuous culture in RPMI 1640 medium supplemented with 10% heat-inactivated fetal calf serum (Irvine Scientific, Santa Ana, CA), penicillin (50 U/ml, Gibco BRL, Grand Island, NY) and streptomycin (50 µg/ml, Gibco BRL). The 3A9 cells were expanded on a 3-day cycle (13).

The ICAM-1/Fc chimera was purchased from R & D Systems, Inc. (Minneapolis, MN). It consisted of all 5 extracellular domains of murine ICAM-1 (Gln 28-Asn 485) and the Fc fragment of human IgG<sub>1</sub>. Antibodies against LFA-1 (i.e., M17/4.2 and FD441.8) and against ICAM-1 (i.e., BE29G1) were purified from culture supernatant by protein G affinity chromatography (1, 13). Stock solutions of PMA (10,000X) (Sigma, St. Louis, MO) were prepared at 1 mM in DMSO.

### Protein immobilization

25 µl of ICAM-1/Fc at 50 µg/ml in 0.1 M NaHCO<sub>3</sub> (pH 8.6) was adsorbed to the center of a 35 mm tissue culture dish (Falcon 353001, Becton Dickinson Labware, Franklin Lakes, NJ) overnight at 4°C. We found that using NaHCO<sub>3</sub> allows for the protein to adhere to the dish better. Unbound ICAM-1/Fc was removed by rinsing the dish three times with PBS. Experiments were done using RPMI 1640 medium supplemented with 10% heat-inactivated fetal calf serum (Irvine Scientific, Santa Ana, CA), penicillin (50 U/ml, Gibco BRL, Grand Island, NY) and streptomycin (50 µg/ml, Gibco BRL). 2ml of the RPMI medium were added to the ICAM-1 coated dish for 30 minutes before the experiment and prior to the addition of 3A9 cells. The fetal calf serum in the medium was used to block the exposed surface of the dish.

### AFM Instrumentation

The AFM that is used in our laboratory is a homemade modification of the standard AFM design that is used for imaging and is shown in Figure 1. In our design, we were able to improve the signal quality by reducing mechanical and electrical noise and improve the instrument's sensitivity by uncoupling the mechanisms for lateral and vertical scans. The cantilever is moved vertically up and down using a piezoelectric translator (Physik Instrumente, model P-821.10) that expands or contracts in response to applied voltage. The vertical range of the piezo is 0-15µm. The dish coated with ICAM-1 is placed below the

cantilever, and the cantilever with a cell attached can be lowered onto that dish using the piezo allowing for the receptor-ligand interaction to take place. During the acquisition of a force scan, the cantilever is bent (Fig. 3) causing the beam of a 3mW diode laser (Oz Optics; em. 680 nm) that is focused on top of the cantilever to be deflected. A 2-segment photodiode (UDT Sensors; model SPOT-2D) monitors these deflections of the laser beam. An 18-bit optically isolated analog-to-digital converter (Instrutech Corp., Port Port Washington, NY) then digitizes the signal from the photodiode. Custom software is used to control the piezoelectric translator and to time the measurements. Our AFM is shielded inside of an acoustic/vibration isolation chamber in order to reduce vibration and aid in keeping a stable temperature. The detection limit of our AFM system is in the range of 20 piconewtons (pN).

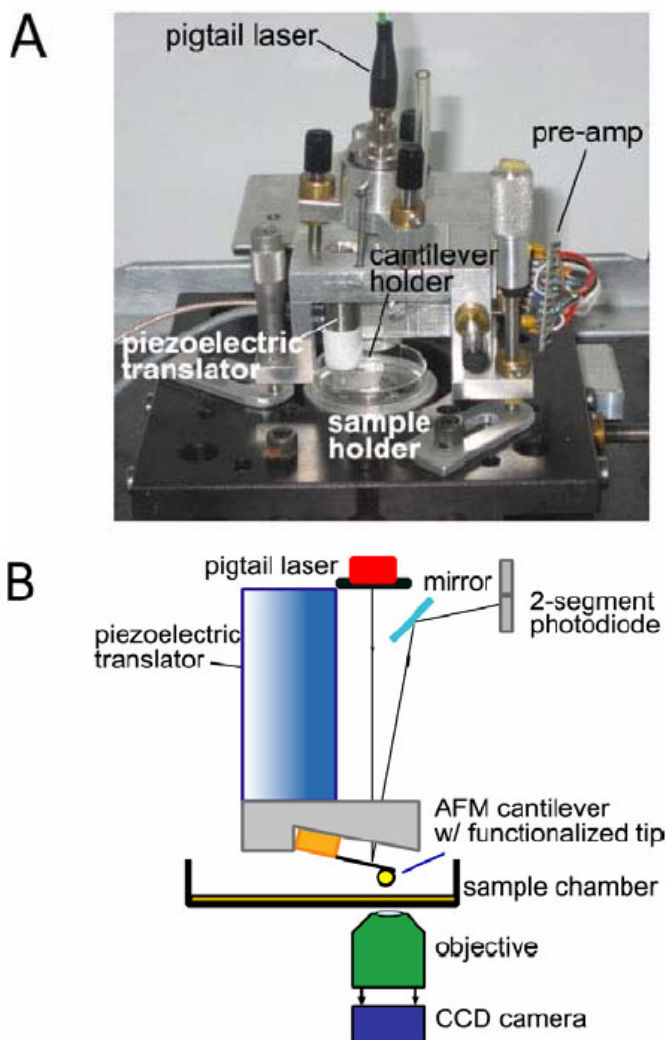


**Fig. 1:** (A) Photograph of our AFM set-up. The CCD camera is not in view. (B) Complete schematic diagram of the AFM.

### AFM measurements of adhesive forces

The AFM force measurements were performed using an AFM apparatus designed to be operated in the force spectroscopy

mode (12-14) (Fig. 1). Concanavalin A (conA)-mediated linkages were used to attach 3A9 cells to the AFM cantilever (3). A schematic representation of this process is shown in Figure 2. The process of cantilever functionalization is described in detail in the protocol section.

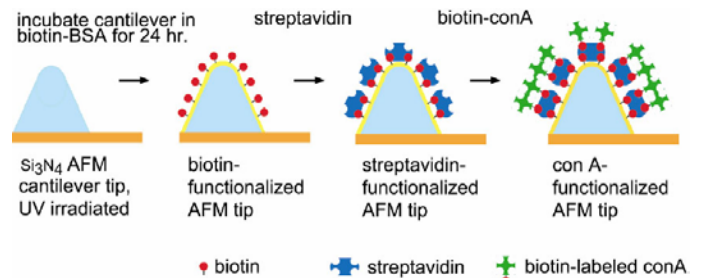


**Fig. 2: Functionalization of an AFM tip with concanavalin A.** Unsharpened  $\text{Si}_3\text{N}_4$  AFM cantilevers were functionalized with biotinylated bovine serum albumin (biotin-BSA) coupled with avidin bound to biotinylated conA.

Our measurements were performed using the largest triangular cantilever ( $320 \mu\text{m}$  long and  $22 \mu\text{m}$  wide) from a set of five on the cantilever chip. These cantilevers were calibrated by analysis of their thermally-induced fluctuation to determine their spring constant (17). Our calibration method is described in detail in the protocol section. The experimentally determined spring constants were consistent with the nominal value of  $10 \text{ mN/m}$  given by the manufacturer.

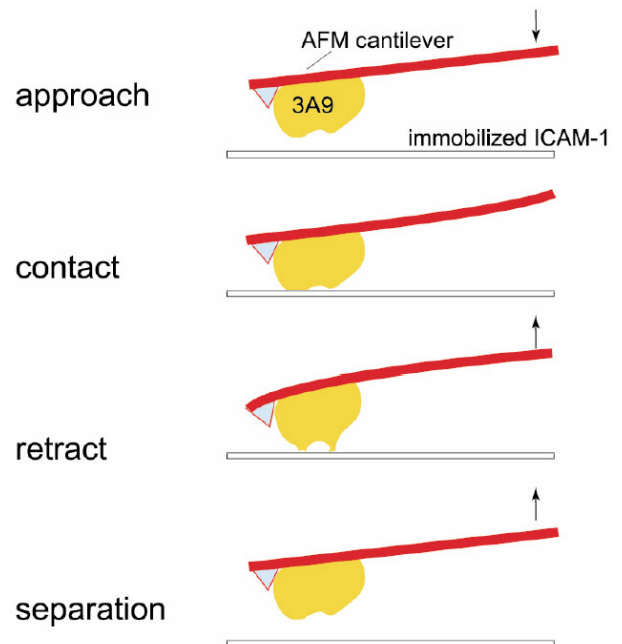


**Fig. 3: Steps in the acquisition of an AFM force measurement.** The first step is the approach of the cantilever with a cell bound to the substrate. This is followed by contact between the cell and substrate and retraction of the cantilever, which results in the separation of the cell from the substrate. The cantilever is bent during this process. The arrows indicate the direction of cantilever movement.

To attach the 3A9 cell to the conA-functionalized cantilever, we began with the light on and the laser off and focused the camera on the cell. At this point, the raised cantilever tip was out of

focus. As the cantilever was lowered and brought closer to the cell of interest, it began to come more into focus. The tip of the cantilever was positioned above the center of a cell and carefully lowered onto the cell for approximately 1 second. It is important to make sure that the cell is behind the AFM tip as lowering the sharp tip onto the cell surface may damage the cell. The moment of contact can be determined visually with the light on or more accurately with the laser on based on the signal from the photodiode. Following contact, the tip was retracted. We were then visually able to determine if the cell had been attached to the cantilever. The attached cell is positioned right behind the AFM tip of the cantilever as is illustrated in Figure 3.

To obtain an estimate of the strength of the cell-cantilever linkage, we allowed the attached cell to interact with a substrate coated with conA for 1 minute. Upon retraction of the cantilever, separation always ( $N > 20$ ) occurred between the cell and the conA-coated surface. The average force needed to induce separation was greater than 2 nN. These measurements revealed that the linkages supporting cell attachment to the cantilever is greater than 2 nN and much larger than the detachment force required to separate the bound 3A9 cell from immobilized ICAM-1 (3).

A piezoelectric translator was used to lower the cantilever/cell onto the sample. The interaction between the attached 3A9 cell and the sample was given by the deflection of the cantilever, which was measured by reflecting a laser beam off the cantilever into a position sensitive 2-segment photodiode detector. AFM cantilevers were purchased from TM Microscopes (Sunnyvale, CA).

### AFM force measurements of individual LFA-1/ICAM-1 complexes

In order to obtain measurements of unitary LFA-1/ICAM-1 unbinding forces, we used conditions that minimized contact between the 3A9 cell and the sample. An adhesion frequency of <30% in the force measurements ensured that there is a >85% probability that the adhesion event is mediated by a single LFA-1/ICAM-1 bond (3).

We corrected all data for hydrodynamic drag. Our determination of the hydrodynamic force was based on the method used by Tees *et al.* (2001) and Evans *et al.* (2001) (18, 19). We allowed the cantilever to undergo free movement at different speeds, and measured the hydrodynamic force for each speed. Our data suggested that the hydrodynamic force acted in the opposite direction of cantilever movement and its magnitude was proportional to the cantilever movement speeds.

### AFM measurements of cell elasticity

The AFM was also used as a microindenter that probes the mechanical properties of the cell. The bare AFM tip was lowered onto the cell surface at a set rate, typically 5  $\mu\text{m/s}$  (Fig. 5B). After contact, the AFM tip exerted a force against the cell that was

proportional to the deflection of the cantilever. The deflection of the cantilever was recorded as a function of the piezoelectric translator position during the approach and withdrawal of the AFM tip. The force-indentation curves of the cells were derived from these records using the surface of the tissue culture dish to calibrate the deflection of the cantilever. Estimates of Young's modulus were made on the assumptions that the cell is an isotropic elastic solid and the AFM tip is a rigid cone (20-22) (Fig. 5A). According to this model, initially proposed by Hertz, the force ( $F$ )-indentation ( $\alpha$ ) relation is a function of Young's modulus of the cell,  $K$ , and the angle formed by the indenter and the plane of the surface,  $\theta$ , as follows:

$$F = \frac{K}{2(1-\nu^2)} \frac{4}{\pi \tan \theta} \alpha^2 \quad (1)$$

We obtained Young's modulus by least square analysis of the force-indentation curves using routines in the Igor Pro (WaveMetrics, Inc., Lake Oswego, OR) software package. We assumed the indenter angle,  $\theta$ , to be  $55^\circ$  and Poisson ratio,  $\nu$ , to be 0.5.

We carried out both cell adhesion and elasticity measurements at  $25^\circ\text{C}$  in fresh tissue culture medium supplemented with 10 mM HEPES buffer. Cells were stimulated by 5 mM  $\text{MgCl}_2$  plus 1 mM EGTA (ethylene glycol-bis- $\beta$ -aminoethylether-N,N,N',N'-tetraacetic acid) or 100 nM phorbol 12-myristate 13-acetate (PMA). The activation of 3A9 by  $\text{Mg}^{2+}$  was immediate. To stimulate the 3A9 cells with PMA, the cells were incubated for ~5 minutes at  $37^\circ\text{C}$  with PMA prior to the start of the experiments. Contact was made with the same cell up to 50 times for a duration of 0.25 seconds and an indentation force of 600 pN in all experiments. We found no dependence on previous contacts in either the elasticity or adhesion AFM studies.

## RESULTS AND DISCUSSION

### AFM force measurements of ligand-receptor interaction

An AFM force measurement of a receptor-ligand interaction between a cell and an opposing substrate coated with ICAM-1 involves four main steps that are shown in Figure 3. First, the cantilever with the 3A9 cell attached is lowered onto an ICAM-1-coated dish. Contact is made, allowing for the receptor-ligand interaction to take place. Then, the cantilever is retracted via the contraction of the piezoelectric translator, pulling the LFA-1/ICAM-1 bonds apart. Finally, complete separation of the two is achieved, and the process can be repeated again. During both the approach and retraction events, the cantilever is bent and the tension between the LFA-1 on the cell and ICAM-1 is determined from the deflection of the cantilever.

AFM studies involving multiple bond interactions provide a wealth of information about a particular receptor-ligand system. The approach trace of the force scan reflects the applied force,

which results in the observed force increase on the graph. As the cantilever is retracted, the bonds formed between LFA-1 and ICAM-1 are stretched until they begin to break, resulting in the saw tooth profile of the force scan. After the last bond is broken, the force returns to zero. Each jump in the force represents one or more LFA-1/ICAM-1 bonds of  $> 50$  pN being broken (Fig. 4A). The maximum force required to dislodge the cell, in our experiments from ICAM-1, is termed the detachment force ( $f_{de}$ ). Another parameter is the work of de-adhesion, which is the work required to stretch the cell and break the LFA-1-ICAM-1 bonds. It is calculated by integrating the adhesive force over the distance traveled by the cantilever. The work of de-adhesion is represented by the shaded area of the first force scan of Figure 4A.

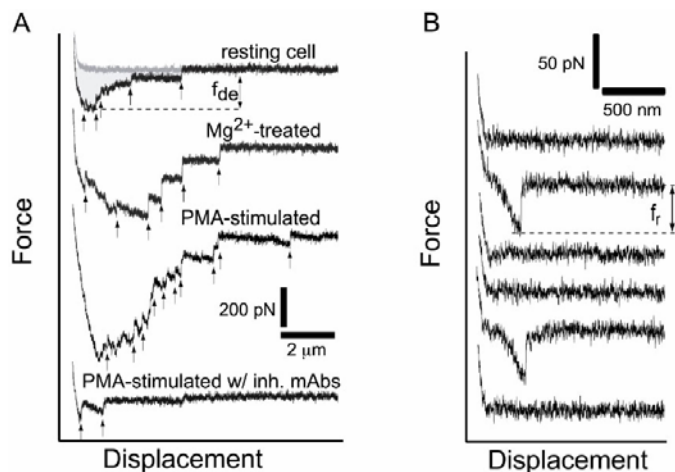


**Fig. 4: AFM force versus displacement traces of the interaction between 3A9 cells and immobilized ICAM-1.** (A) Multiple-bond measurements acquired with a compression force of 200 pN, 5 seconds contact and a cantilever retraction speed of 2 μm/second. The measurements were carried out with a resting cell (1st trace), a Mg<sup>2+</sup>-treated cell (2nd trace), and a PMA-stimulated cell (3rd trace). The 4th trace corresponds to a measurement acquired from a PMA-stimulated cell in the presence of LFA-1 (20 μg/ml FD441.8) and ICAM-1 (20 μg/ml BE29G1) function-blocking monoclonal antibodies (mAbs). Arrows point to breakage of LFA-1/ICAM-1 bond(s).  $f_{de}$  is the detachment force and the shaded area estimates the work of de-adhesion. (B) Single-molecule measurements of LFA-1/ICAM-1 unbinding forces. Traces 2 and 5 show adhesion. Measurements were obtained under conditions that minimized contact between the 3A9 cell and the ICAM-1 coated surface. The compression force was reduced to ~60 pN and the contact time to 50 milliseconds. An adhesion frequency of less than 30% in the force measurements ensured that there is a  $>85\%$  probability that the adhesion event is mediated by a single LFA-1/ICAM-1 complex (18). The frequency of adhesion in test and control experiments was examined to confirm the specificity of the interaction (18, 19). The addition of monoclonal antibodies against either LFA-1 or ICAM-1 significantly lowered the frequency of adhesion of both resting and activated cells under identical experimental conditions. Both resting and stimulated 3A9 cells exhibited lower frequency of adhesion to immobilized bovine albumin than to immobilized ICAM-1.

The parameters mentioned above allow us to determine changes in adhesion. Both the compression force and contact time have an impact on adhesion. For example, a greater compression force and a longer time of contact will result in greater adhesion. Adhesion can also be modulated by cell activation. The force scan of a resting cell has fewer bonds formed and a smaller area of de-adhesion and detachment force than force scans of cells treated with agents promoting adhesion. We used Mg<sup>2+</sup>, which has been found to activate LFA-1 (23, 24). The result of Mg<sup>2+</sup>

activation is an increase in the number of bonds formed between the two complexes and in the work of de-adhesion and detachment force (Fig. 4A) (2, 3). We also stimulated the cells using phorbol- myristate acetate (PMA). It activates a protein kinase C pathway that leads to enhanced adhesion (25-27). With this agent, we see an even greater increase in the number of bonds formed as well as a great increase in the work of de-adhesion and detachment force (Fig. 4A) (2, 3). It is essential to confirm the specificity of any interaction. For the LFA-1/ICAM-1 interaction, this can be done with readily available antibodies for both LFA-1 and ICAM-1. The last force scan of Figure 4A represents an ICAM-1/LFA-1 interaction that had been blocked with an antibody. After blocking both the ligand and receptor, almost all adhesion is eliminated (2, 3).

### AFM measurements of individual complexes

The AFM allows us to examine single molecule interactions. There is a greater than 85% chance that a single molecule interaction is being measured if the adhesion frequency is reduced to less than 30%. This is achieved by reducing both the duration of contact between the cell and ICAM-1 as well as the applied compression force. In the ICAM-1/LFA-1 experiments contact was reduced to ~50ms and the compression force to ~60pN.

Single molecule measurements can be seen in Figure 4B. Adhesion only takes place in the second and fifth force scans, and it is a single molecule breakage. The unbinding force is calculated from the magnitude of the force transition with corrections for hydrodynamic drag. In order to determine the force versus loading rate profile, the force spectra were first plotted versus piezo displacement. Loading rates were obtained by multiplying the slope of the force versus displacement curve with the retraction speed of the cantilever. The resulting force versus loading rate relationship always showed an increase of unbinding force with increasing loading rate (2, 3).

### AFM elasticity measurements

The mechanical properties of the cell were determined through AFM indentation measurements of cell compliance. The indentation force used was below 1nN (~600 pN). In order to satisfy the constraints of the Hertz model, it is important to consider indentations of less than 10% of the diameter of the cell (28). The 3A9 cells used in our studies were between 10-15 μm in diameter. Therefore, we only considered indentations of less than 1 μm.

In order to determine the cell's elasticity, the force versus indentation measurements were fitted to the curves of the Hertz model (Fig. 5C). In our experiments it was important to determine the elasticity of the 3A9 cells in the different conditions that were used for activating the cells. We found that the cells treated with PMA had the lowest Young's modulus values and were, therefore, the most compliant. This would lead to a greater degree of spreading by these cells during AFM force measurements and offered an explanation for the large work of



de-adhesion that was observed with the force scans of the PMA-treated cells (Fig. 5D) (2).

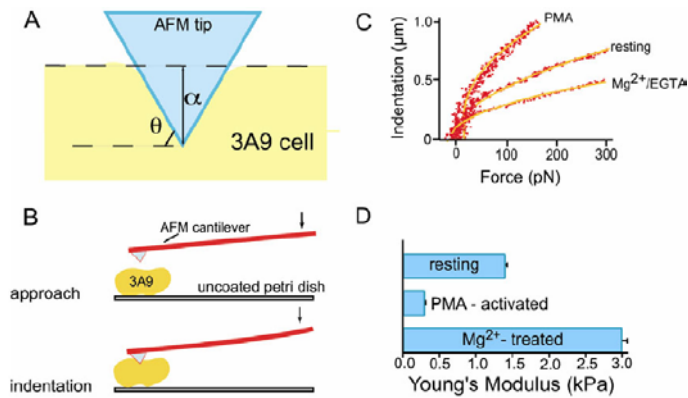


**Fig. 5: Acquisition of cell compliance measurements.** (A) Tip of the AFM cantilever indenting a 3A9 cell. The cell compliance measurements were based on the assumption that the cell is an isotropic elastic solid and the AFM tip is a rigid cone (20-22). According to this model, initially proposed by Love and Hertz, the force ( $F$ ) -indentation ( $\alpha$ ) relation (shown) is a function of Young's modulus of the cell,  $K$ , and the angle formed by the indenter and the plane of the surface,  $\theta$ , as follows:

$$F = \frac{K}{2(1-\nu^2)} \frac{4}{\pi \tan \theta} \alpha^3 \quad (1)$$

We assumed the indenter angle,  $\theta$ , formed by the AFM tip and the 3A9 cell to be  $55^\circ$  and Poisson ratio,  $\nu$ , to be 0.5. (B) Schematic of an AFM cell compliance measurement. During the approach, the cantilever is lowered onto the center of a 3A9 cell. Then the cell is indented with the tip of the cantilever. Arrows indicate direction of cantilever movement. (C) Force versus indentation traces of resting, PMA-stimulated and  $\text{Mg}^{2+}$ -treated 3A9 cells. (D) Young's modulus of resting, PMA-stimulated and  $\text{Mg}^{2+}$ -treated 3A9 cells. The data is based on 15-30 elasticity measurements per cell done on 25 different 3A9 cells in each case. The error bar is the standard error.

## Calibration

Obtaining the right values for the cantilever spring constant and slope is critical for correct data analysis. Our calibration procedure is described in the protocol section below. It is best to perform the calibration prior to picking up the cell and carrying out an experiment for a couple of reasons. After a cell has been attached to the cantilever tip, it may leave debris on the cantilever that may alter the slope due to the excess material on the tip. Secondly, it is crucial to obtain the calibration numbers prior to beginning the experiment since the cantilever may become damaged during the course of the experiment. If this occurs, then one can no longer perform the calibration and the data cannot be analyzed. Lastly, the obtained slope and spring values can reveal possible cantilever damage. Sometimes one arm of the cantilever can be damaged/cracked. This type of damage can escape a visual inspection of the cantilever and may interfere with results. For example, the cantilevers we use typically have a spring constant of 10 mN/m. If the spring constant is 4 mN/m, one can assume that that particular cantilever has sustained some damage.

## AFM set-up

Outside noise can severely interfere with obtaining data. In order to block out acoustical and mechanical noise, our set-ups are

shielded inside of acoustic/vibration isolation chambers. This also aids in maintaining the temperature. For our experiments it is important to keep the temperature above  $25^\circ\text{C}$  to keep the cells alive.

## Attaching cells to the AFM cantilever

As described in the methods and protocol sections, cells were attached via biotin- BSA, streptavidin, and finally concanavalin A (conA) as is presented in Figure 2. The cells used in these types of AFM experiments must have surface receptors for conA for the described method of attachment. We use 3A9 and K562 cells in our experiments.

The strength of the conA attachment is many times stronger than the interaction of LFA-1 and ICAM-1 (2nN versus 50 pN). This is crucial for these types of measurements because if the receptor/ ligand interaction being studied is stronger than the conA linkage, then the cell will come off the tip. If this should occur one will only observe one measurement resulting from the conA linkage breaking. Normally, we are able to obtain hundreds of measurements on the LFA-1/ ICAM-1 system without the cell coming off the cantilever tip.

When attaching a cell to the cantilever, it is best to keep the concentration of cells in the tissue culture dish low enough so that there are only a few cells in the field of vision. This makes it easier to determine whether a cell had attached to the cantilever. Also, a high cell concentration can increase the likelihood of an extra cell attaching to the cantilever tip, which could interfere with results. The extra cells can also stick to the cell that is already attached to the cantilever. In this case, the measurements would be complicated by cell to cell interactions that would be recorded in addition to the interaction of the cell with the protein substrate on the bottom of the dish.

## Elasticity measurements

During elasticity measurements, the cell surface is probed with the cantilever tip. In our experiments, we had used 3A9 cells that are  $10 \mu\text{m}$  in diameter. Using considerably smaller cell types could be difficult. It is important to probe the center of the cell with the cantilever tip, as the cell can very often slip out from under the cantilever. One must continuously make sure that the tip is still touching the cell and not the surface of the tissue culture dish. Probing the dish surface will result in extremely high Young's modulus values, as the dish is much stiffer than a cell. To avoid this, it is best to turn off the laser every few measurements and turn on the light to clearly inspect the position of the cantilever. Often, it may be helpful to do a few measurements with the light on in order to visualize the path of the cantilever and where it is touching the cell surface. If the tip is touching the cell considerably off-center, the cell is more likely to slip out from under the cantilever.

Learning how to operate the AFM can take more time than performing a simple adhesion assay for the first time. However, there are many benefits to adapting this technique. The AFM is a

versatile tool that can be used to study cell adhesion as well as cell compliance. As we described, cell adhesion studies can be performed at both the multiple bond and the single molecule level providing a wealth of information about a particular receptor-ligand system. Cell compliance studies can complement the adhesion studies with information concerning the mechanical properties of the cell.

## ACKNOWLEDGEMENTS

We thank C. Freitas and Dr. Aileen Chen for technical support. This work was supported by grants from the American Cancer Society, and the NIH (GM55611). XZ is supported by a predoctoral fellowship from the AHA.

The authors have no conflicts of interest to declare related to this publication.

## REFERENCES

- Sanchez-Madrid F, Simon P, Thompson S, Springer TA. Mapping of antigenic and functional epitopes on the alpha- and beta-subunits of two related mouse glycoproteins involved in cell interactions, LFA-1 and Mac-1. *J Exp Med* 1983; 158(2):586-602.
- Wojcikiewicz EP, Zhang X, Chen A, Moy VT. Contributions of molecular binding events and cellular compliance to the modulation of leukocyte adhesion. *Journal of Cell Science* 2003; 116(12):2531-2539.
- Zhang X, Wojcikiewicz E, Moy VT. Force spectroscopy of the leukocyte function-associated antigen-1/intercellular adhesion molecule-1 interaction. *Biophys J* 2002; 83(4):2270-2279.
- Binnig G, Quate CF, Gerber C. Atomic force microscope. *Phys Rev Lett* 1986; 56:930-933.
- Lee GU, Kidwell DA, Colton RJ. Sensing discrete streptavidin-biotin interactions with AFM. *Langmuir* 1994; 10(2):354-361.
- Oesterhelt F, Oesterhelt D, Pfeiffer M, Engel A, Gaub HE, Muller DJ. Unfolding pathways of individual bacteriorhodopsins. *Science* 2000; 288(5463):143-146.
- Rief M, Gautel M, Oesterhelt F, Fernandez JM, Gaub HE. Reversible unfolding of individual titin immunoglobulin domains by AFM. *Science* 1997; 276(5315):1109-1112.
- Bell GI. Models for the specific adhesion of cells to cells. *Science* 1978; 200:618-627.
- Evans E, Ritchie K, Merkel R. Sensitive technique to probe molecular adhesion and structural linkages at biological interfaces. *Biophys J* 1995; 68:2580-2587.
- Merkel R, Nassoy P, Leung A, Ritchie K, Evans E. Energy landscapes of receptor-ligand bonds explored with dynamic force spectroscopy. *Nature* 1999; 397(6714):50-53.
- Yuan C, Chen A, Kolb P, Moy VT. Energy landscape of streptavidin-biotin complexes measured by atomic force microscopy. *Biochemistry* 2000; 39(33):10219-10223.
- Benoit M. Cell adhesion measured by force spectroscopy on living cells. *Methods Cell Biol* 2002; 68:91-114.
- Kuhlman P, Moy VT, Lollo BA, Brian AA. The accessory function of murine intercellular adhesion molecule-1 in T lymphocyte activation. Contributions of adhesion and co-activation. *J Immunol* 1991; 146(6):1773-1782.
- Benoit M, Gabriel D, Gerisch G, Gaub HE. Discrete interactions in cell adhesion measured by single-molecule force spectroscopy. *Nat Cell Biol* 2000; 2(6):313-317.
- Heinz WF, Hoh JH. Spatially resolved force spectroscopy of biological surfaces using the atomic force microscope. *Trends Biotechnol* 1999; 17(4):143-150.
- Willemsen OH, Snel MM, Cambi A, Greve J, De Grooth BG, Figdor CG. Biomolecular interactions measured by atomic force microscopy. *Biophys J* 2000; 79(6):3267-3281.
- Hutter JL, Bechhoefer J. Calibration of atomic-force microscope tips. *Rev Sci Instrum* 1993; 64(7):1868-1873.
- Tees DFJ, Woodward JT, Hammer DA. Reliability theory for receptor-ligand bond dissociation. *J Chem Phys* 2001; 114:7483-7496.
- Evans E. Probing the relation between force-lifetime-and chemistry in single molecular bonds. *Annual Review of Biophysics & Biomolecular Structure* 2001; 30:105-128.
- Hoh JH, Schoenenberger CA. Surface morphology and mechanical properties of MDCK monolayers by atomic force microscopy. *J Cell Sci* 1994; 107:1105-1114.
- Radmacher M, Fritz M, Kacher CM, Cleveland JP, Hansma PK. Measuring the viscoelastic properties of human platelets with the atomic force microscope. *Biophys J* 1996; 70(1):556-567.
- Wu HW, Kuhn T, Moy VT. Mechanical properties of L929 cells measured by atomic force microscopy: effects of anticytoskeletal drugs and membrane crosslinking. *Scanning* 1998; 20(5):389-397.
- Ganpule G, Knorr R, Miller JM, Carron CP, Dustin ML. Low affinity of cell surface lymphocyte function-associated antigen-1 (LFA-1) generates selectivity for cell-cell interactions. *Journal of Immunology* 1997; 159(6):2685-2692.
- Huth JR, Olejniczak ET, Mendoza R, Liang H, Harris EA, Lupper ML Jr., Wilson AE, Fesik SW, Staunton DE. NMR and mutagenesis evidence for an I domain allosteric site that regulates lymphocyte function-associated antigen 1 ligand binding. *Proc Natl Acad Sci USA* 2000; 97(10):5231-5236.
- van Kooyk Y, Figdor CG. Avidity regulation of integrins: the driving force in leukocyte adhesion. *Curr Opin Cell Biol* 2000; 12(5):542-547.
- Zhou X, Li J. Macrophage-enriched myristoylated alanine-rich C kinase substrate and its phosphorylation is required for the phorbol ester-stimulated diffusion of beta 2 integrin molecules. *J Biol Chem* 2000; 275(26):20217-20222.

27. Jones SL, Wang J, Turck CW, Brown EJ. A role for the actinbundling protein L-plastin in the regulation of leukocyte integrin function. *Proc Natl Acad Sci USA* 1998; 95(16):9331-9336.
28. Costa KD, Yin FC. Analysis of indentation: implications for measuring mechanical properties with atomic force microscopy. *Journal of Biomechanical Engineering* 1999; 121(5):462-471.
29. Sader JE. Parallel beam approximation for V-shaped atomic force microscope cantilevers. *Rev Sci Instrum* 1995; 66:4583-4587.
30. Senden TJ, Ducker WA. Experimental determination of spring constants in atomic force microscopy. *Langmuir* 1994; 10:1003-1004.



## PROTOCOLS

### A. Cantilever functionalization for use in experiments with living cell

The following outlines a method for functionalizing tips with biotin-BSA and streptavidin followed by concanavalin A (Fig. 2). This method is advantageous since the streptavidin/biotin system has been well characterized, is high-affinity, and the initial layer of biotin-BSA may help to mask any electrical charges on the cantilever tip that could lead to nonspecific binding. Materials: AFM cantilevers (MLCT-AUHW, Veeco Instruments, Sunnyvale, CA), biotin-BSA (A-6043, Sigma, St. Louis, MO), streptavidin (Sigma), and biotinylated concanavalin A (biotin-conA) (Sigma).

1. Soak cantilever for 5 min. in acetone and then UV irradiate for 15 min.
2. Incubate cantilever in a 50  $\mu$ l drop of biotin-BSA (0.5 mg/ml in 0.1 M sodium bicarbonate, pH 8.6; Sigma) overnight at 37°C in a humidified incubator.
3. Wash cantilever three times in phosphate buffered saline (PBS, 10 mM  $\text{PO}_4^{3-}$ , 150 mM NaCl, pH 7.3) to remove unbound protein (NOTE: At this point cantilevers can be stored in PBS at 4°C for up to a week).
4. Incubate cantilever in a 50  $\mu$ l drop of streptavidin (0.5 mg/ml in 0.01 M PBS, pH 7.3, Pierce, Rockford, IL) for 10 min. at room temperature.
5. Wash cantilever 3x in PBS.
6. Incubate cantilever in biotin-conA (0.2 mg/ml in PBS, Sigma) for 10 minutes at room temperature.
7. Wash cantilever 3x in PBS.

Note: It is important that biotin-BSA adsorption takes place at pH 8.3 or higher, as the basic conditions seem to facilitate BSA adsorption to the cantilever.

### B. Cantilever Calibration

It is necessary to determine the spring constant of the cantilever,  $k_C$  (i.e.,  $F = k_C x$ ) in order to translate the deflection of the cantilever,  $x$ , to units of force,  $F$ . Calibrating the cantilever can be achieved through theoretical techniques that provide an approximation of  $k_C$  (29) or through empirical methods. Using empirical methods to determine  $k_C$  involves taking measurements of cantilever deflection with application of a constant known force (30) or measuring the cantilever's resonant frequency (17). The method we use for calibrating cantilevers is based on Hutter and Bechhoefer. We use triangle-shaped unsharpened gold-coated silicon-nitride cantilever tips that have spring constants ranging from 10 mN/m to 50 mN/m for ligand-receptor force measurements. The cantilever tip can be treated as a simple harmonic oscillator whose power spectrum of thermal fluctuation can be used to derive the spring constant. This can be achieved by raising the cantilever a few microns from the surface of the experimental dish and monitoring its natural vibrational frequency for 2-3 seconds. Each vibration mode of the cantilever receives the thermal energy commensurate to one degree of freedom,  $k_B T/2$ . The measured variance of the deflection  $\langle x \rangle^2$ , can then be used to calculate the spring constant (i.e.,  $k_B T = k_C \langle x \rangle^2$ , where  $k_B$  and  $T$  are Boltzmann's constant and temperature, respectively). To separate deflections belonging to the basic (and predominant) mode of vibration from other deflections or noise in the recording system, the power spectral density of the temperature-induced deflection is determined. The spring constant is estimated using only the spectral component corresponding to the basal mode of vibration. The spring constant can be calibrated in either air or solution using this approach. The calculated spring constant  $k_C$  can then be used to calculate rupture force,  $F$ , by  $F = k_C \Delta V$ .  $\Delta V$  is the change in voltage detected by the photodiode just prior to and immediately after the rupture event.  $C$  is a calibration constant that relates deflection and photodiode voltage and is determined from the deflection of the cantilever when it is pressed against a rigid surface, such as the bottom of a plastic petri dish.